

## SURFACE SELF-ORDERING IN OBLIQUELY DEPOSITED $As_2S_3$ FILMS

M. V. Sopinsky\*, V. I. Mynko, I.Z. Indutnyi, O. S. Lytvyn, P.E Shepeliavyi.  
*V Lashkaryov Institute of Semiconductor Physics, NASU, 45, Prospekt Nauky, Kyiv,  
Ukraine, 03028*

The surface morphology of 250-3000 nm thick  $As_2S_3$  films vacuum deposited within 70-80° scale of vapor incidence angles is studied by AFM. It is observed that the surface relief of obliquely deposited films (ODF) shows quasi-regular grating-like structure, with the spatial frequency of quasi-gratings being in the 500-6000  $mm^{-1}$  range, and relief depth of up to 60 nm. The influence of the film thickness and the type of the substrate on the surface morphology is demonstrated. The most probable explanation for the observed surface effect is the near-surface stress that plays significant role in the self-organized ordering of nanostructures at the mesoscopic length scales (from several nanometers to hundreds of nanometers).

(Received September 24, 2008; accepted October 1, 2008)

*Keywords:* obliquely deposited films, surface wrinkles,  $As_2S_3$ , self-ordering

### 1. Introduction

As amorphous chalcogenide vacuum-deposited films have high degree in the non-equilibrium state, their physical and chemical properties are very sensitive to the conditions of formation. In spite of this circumstance rather little work has been done [1-12] to study the properties of obliquely deposited chalcogenide films. It was established that these films are characterized by a columnar structure and a granular surface morphology [1-12]. Both the surface and internal microstructure are strongly influenced by the vapour incidence angle, i.e. the angle between the vapour beam direction and the substrate normal. Increasing the latter leads to a considerable change in the optical, mechanical and other structure related properties of the films [1-12].

Most of those papers are devoted to the investigation of Ge-based chalcogenides as morphological changes caused by oblique deposition are more pronounced in films of these compounds.

In this paper we present our first results on the surface morphology studies for  $As_2S_3$  films thermally evaporated within 70-80° range of the vapour incidence angles.

### 2. Experimental procedure

The experiments were performed with as-deposited  $As_2S_3$  films, 250-3000 nm thick, obtained with conventional rotary and oil diffusion pumps maintaining residual pressure in the order of  $(1-3) \times 10^{-3}$  Pa. High purity  $As_2S_3$  glass placed in tantalum boat was used for evaporation. The substrates were cleaned glass plates – bare and covered by thin (20-80 nm) film of vacuum deposited chromium, as well as cleaned Si (111) wafers. During the evaporation process, the substrate temperature was close to the surrounding room. The substrate were oriented at the angles within  $\beta = 70-80^\circ$  and  $\beta = 0^\circ$  between the normal to the substrate surface and the direction to the evaporator. The deposition rate was  $\sim 1-2$  nm/s, as controlled by the quartz microbalance. The distance between the evaporation source and substrate center was always 22 cm.

The investigations of the films' surfaces were performed in air with the Nanoscope IIIa multimode atomic force microscope (Veeco Instruments Inc.). The semi-contact resonance regime ("tapping" mode) was used to image the topographic features of the samples. The AFM probes were commercially available ultra-

---

\*Corresponding author: [sopinsky@isp.kiev.ua](mailto:sopinsky@isp.kiev.ua)

sharp silicon tips (RTESP, Veeco Instruments) with the radius of curvature of less than 10 nm. Imaging conditions were chosen to minimize the sample damage and optimize image clarity.

Multi-angle ellipsometric measurements have been performed to determine the thickness and refractive index of the films. The measurements were done using PCSA null type ellipsometer LEF-3M-1 (Feodosia, Ukraine) equipped with He-Ne laser as a light source ( $\lambda = 632.8$  nm).

### 3. Experimental results

AFM patterns show the difference of the surface morphology of obliquely deposited  $\text{As}_2\text{S}_3$  films (ODF) as compared to the normally deposited films (NDF) - well-aligned protrusions and depressions in the film surface, with their orientation being perpendicular to the incidence plane of vapor beam are observed in ODF.

Fig 1a shows the surface morphology of the 540-nm-thick  $\text{As}_2\text{S}_3$  film, deposited on the glass substrate over the 20 nm chromium film. Section analysis of the surface's topology is given in Fig. 1b. The Power Spectral Density (PSD) function of NanoScope software has also been used. It is useful in analyzing surface roughness. This function provides a representation of the amplitude of a surface's roughness as a function of the spatial frequency of the roughness. Spatial frequency is the inverse of the wavelength of the roughness features. As can be seen from the figure, the spatial frequency spectrum is rather narrow and has the prevailing frequency with the highest amplitude (at the frequency of  $\nu = 4.4/\mu\text{m}$ ). Thus, the surface of the film may be considered as quasi-grating with the period of 227 nm. The grating have relief depth of  $\sim 2$  nm and depth modulation ((relief depth)/period ratio)  $\sim 0.01$ .

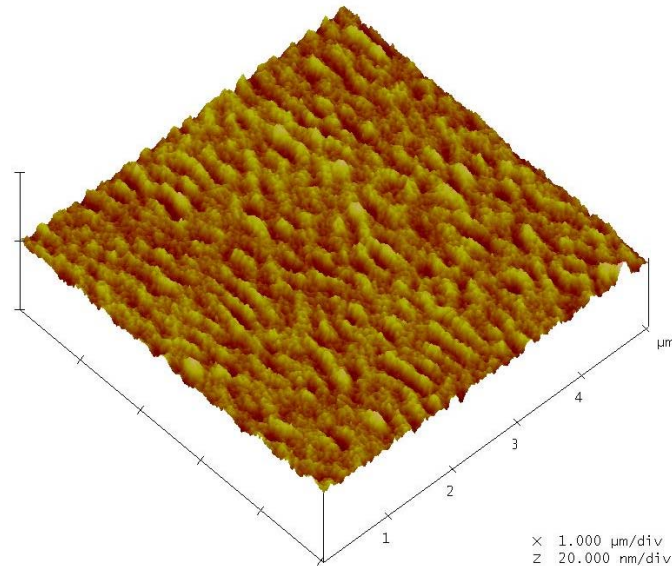


Fig. 1a.

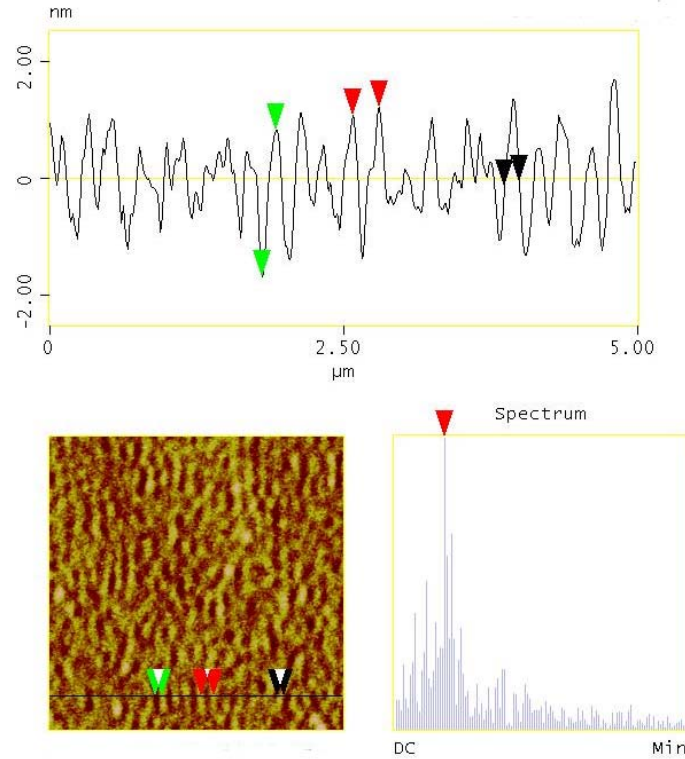


Fig. 1b.

Fig. 1. Surface picture (a), section analysis and PSD function (b) for the 540 nm thick  $\text{As}_2\text{S}_3$  film on glass-Cr substrate.

AFM patterns of several ODF on various substrates have shown that in all cases the surface of the films may be considered as quasigrating structure with the ridges aligned in the direction perpendicular to the vapor beam incidence plane. The main factor determining the characteristics of quasigrating structure of the film surface is the thickness of the films. The following change in surface morphology with the increase of film thickness was obtained:

- All the spatial frequency spectra have the strong lines with the spatial frequency  $\nu_1 = 4 - 6$  lines per  $\mu\text{m}$ .

- As the film thickness increases, so do the line amplitudes with the spatial frequencies under  $\nu_1$ .

- For films with thickness  $\geq 740$  nm, two prevailing spatial frequencies that differ by approximately an order of magnitude are observed:  $\nu_1 \sim 5/\mu\text{m}$ , with the amplitude ( $A1$ ), and  $\nu_2 \sim 0.5/\mu\text{m}$ , with ( $A2$ ).

As the thickness of film increases, the ratio of spectral amplitudes  $A2/A1$  increases as well. As it has been noted above, at  $l = 540$  nm the quasigrating with spatial frequency of  $\nu_1 = 4.4/\mu\text{m}$  is the dominant pattern in surface roughness. However, at  $l = 740$  nm  $A2$  is nearly equal to  $A1$  – the envelope amplitude of low-frequency grating is 1.5-2.0 nm, and the relief height of high-frequency grating is 2.5 nm. At  $l = 1450$  nm the  $A2$  already exceeds the  $A1$  – the envelope amplitude of low-frequency grating is  $\sim 45$  nm, and relief height of high-frequency grating is 15-60 nm. At  $l = 2160$  nm the  $A2/A1$  is equal  $65\text{nm}/28\text{nm} \approx 2.3$ .

Thus, the major regularities that manifest themselves with the film thickness increase are:

- significant growth of relief depth;
- minor change of spatial frequency of high-frequency grating;
- increase of modulation of high-frequency grating by low-frequency grating.

The type of substrate is yet another factor that defines the characteristics of the  $\text{As}_2\text{S}_3$  films. First of all, there has been found the systematic difference between the thickness of the films simultaneously deposited on the surface of bare and chromium-layer-covered glass substrates. The ratio  $l(\text{glass})/l(\text{glass+Cr})$  itself was 1.15-1.22 (where  $l(\text{glass})$  – thickness of  $\text{As}_2\text{S}_3$  film on glass substrate,  $l(\text{glass+Cr})$  – thickness of  $\text{As}_2\text{S}_3$  film on

glass substrate covered by Cr layer). The film thickness was measured using both AFM and ellipsometrical methods. It should be emphasized that the values of film thickness calculated from ellipsometric measurements are very close to those obtained by the AFM, within 10-20 nm from each other. This fact confirms the reliability of the presented results.

Such a noticeable difference in the film thickness depending on the substrate material can be caused by different sticking coefficients and/or different film density. Ellipsometrical results for the oblique deposited  $\text{As}_2\text{S}_3$  films on various substrates don't show the sufficient difference in the refractive index values. Thus, the observed difference in the film thickness is primarily caused by the different values of sticking coefficient. The sticking coefficient for oblique deposition of  $\text{As}_2\text{S}_3$  films on Cr is lower as compared to the deposition on glass.

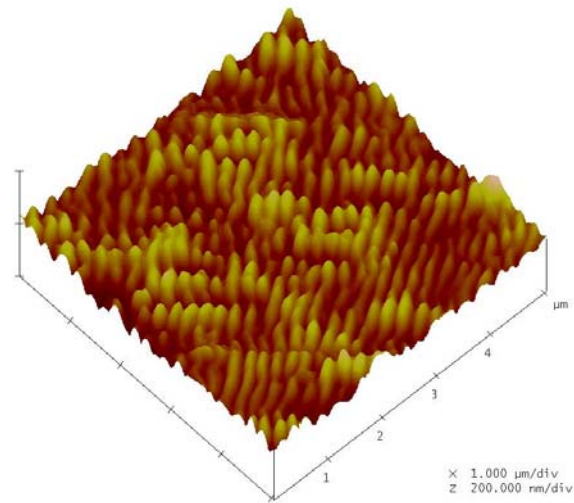


Fig. 2a.

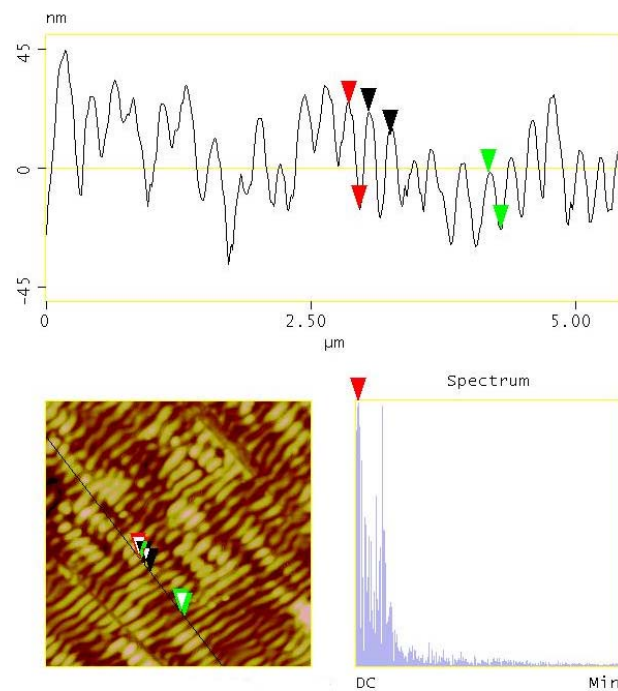


Fig. 2b.

Fig. 2. Surface picture (a), section analysis and PSD function (b) for the 1600 nm thick  $\text{As}_2\text{S}_3$  film on glass substrate.

However, the substrate also influences the surface structure ordering to some degree. The preliminary deposition of polycrystalline Cr layer on glass substrate results in the better self-ordering of the  $\text{As}_2\text{S}_3$  film surface. This can be illustrated by the AFM-data obtained for the  $\sim 1500$  nm thick  $\text{As}_2\text{S}_3$  films deposited on the bare and Cr-covered glass substrates (Figure 2 for the film on glass and Figure 3 for glass + Cr). Better ordering of the film surface has been observed for the film deposited on the Cr-covered glass substrate as compared to the one deposited directly on glass. The elongated surface ridges for the film on bare glass are broken into the shorter sections lengthwise.

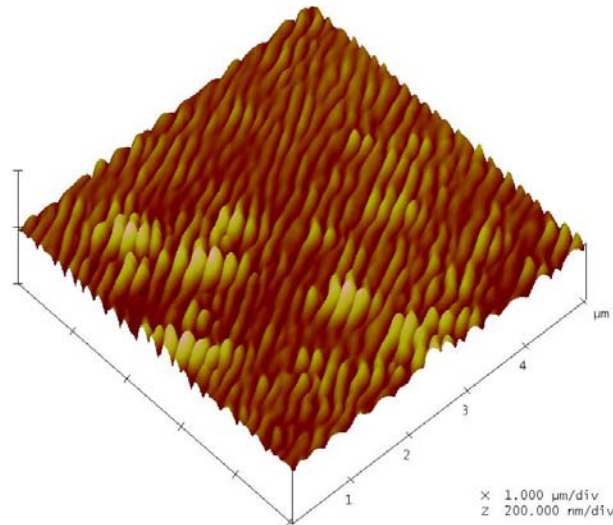


Fig. 3a.

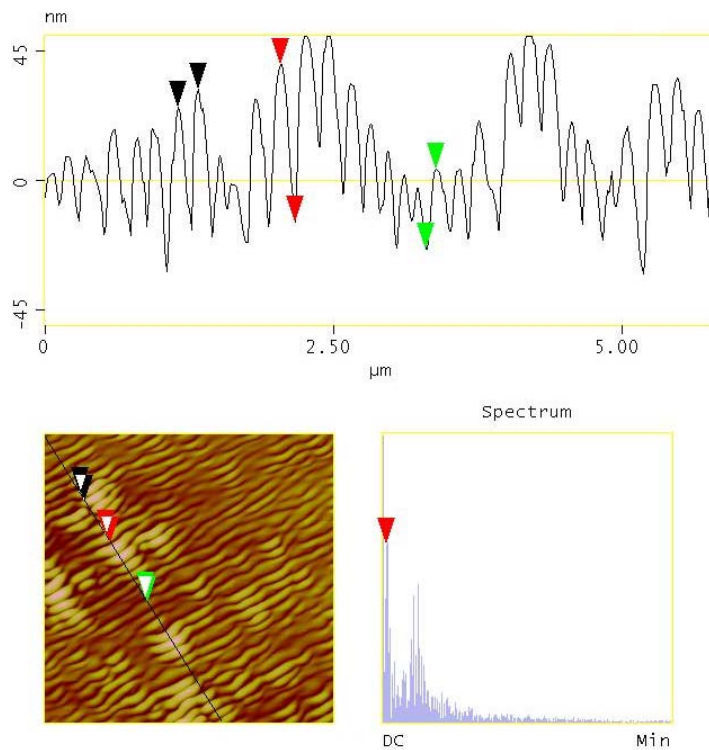


Fig. 3b.

Fig. 3. Surface picture (a), section analysis and PSD function (b) for the 1450 nm thick  $\text{As}_2\text{S}_3$  film on glass-Cr substrate.

The PSD function shows that the surface spatial spectra of both films have two prevailing spatial frequencies with highest amplitudes. They are  $\nu_1 \sim 5.71/\mu\text{m}$  and  $\nu_2 \sim 0.515/\mu\text{m}$  for the film on Cr-covered;  $\nu_1 \sim 5.00/\mu\text{m}$  and  $\nu_2 \sim 0.367/\mu\text{m}$  on the bare glass. Main difference between the films' surfaces spectra consists in higher amplitudes for the intermediate noise frequencies between  $\nu_1$  and  $\nu_2$  for the film on bare glass. This fact right reflects the lower degree of its surface ordering.

Ellipsometry also provides some information on the macrostructure of the obliquely deposited  $\text{As}_2\text{S}_3$  films. Refractive index ( $n$ ) values calculated according to the framework of the "isotropic uniform layer model" are lower in these films as compared to the values for the films with the normal (perpendicular) deposition. The difference is several hundredths: the values of 2.38-2.44 are found for our obliquely deposited  $\text{As}_2\text{S}_3$  films and the values of 2.45-2.50 are found for our perpendicularly deposited  $\text{As}_2\text{S}_3$  films. Our values of  $n$  are close to the values obtained in [9] where for 1500 nm thick  $\text{As}_2\text{S}_3$  films the refractive index at  $\lambda = 633$  nm was 2.475 for  $\beta = 0^\circ$  and 2.385 for  $\beta = 70^\circ$ . Thus, compactness of obliquely deposited  $\text{As}_2\text{S}_3$  films is lower compared to the normally deposited  $\text{As}_2\text{S}_3$  films. However, this decrease in density in  $\text{As}_2\text{S}_3$  films due to oblique deposition (several percentage points) is considerably less pronounced as compared to the obliquely deposited films with low mobility of adatoms. For example, in  $\text{SiO}_x$  films [13] the porosity exceeds 50%.

Ellipsometrical data show that at the same deposition angle the refractive index of the obliquely deposited  $\text{As}_2\text{S}_3$  film decreases with the increase of the film thickness. This fact confirms the increase of films' porosity with thickness. For the perpendicularly deposited  $\text{As}_2\text{S}_3$  films the opposite effect takes place - the refractive index increases with film thickness. Thus, the difference between the refractive index values for obliquely and perpendicularly deposited  $\text{As}_2\text{S}_3$  films of the equal thickness increases with the increase in film thickness.

#### 4. Discussion

The mechanism of formation of the observed surface patterns in obliquely deposited  $\text{As}_2\text{S}_3$  films is not yet well understood. Ordered oriented surface structure may be the result of the formation of row-like column aggregates in the direction perpendicular to the plane of incidence as it has been observed in thin amorphous metallic films deposited at large angle [14]. Since the columnar structure is reflected in the topography of the top surface of the films in such a way that the columns are revealed as protrusions, and the low-density network as depressions in the films surface, the above mentioned aggregation can lead to the formation of 1D-quasigrating surface pattern in such films. However, strictly ordered column-like structure is only observed for thin films with low mobility of adatoms. The  $\text{As}_2\text{S}_3$  films investigated here don't conform to those criteria.

The morphology of obliquely deposited 5-1500 nm thick  $\text{As}_2\text{S}_3$  films was studied in [6, 7] by conventional transmission and scanning electron microscopy in order to reveal their surface microstructure and growth morphology. The results have shown that vacuum deposited thin films of a- $\text{As}_2\text{S}_3$  are characterized by columnar structure and granular surface morphology. The surface granular structure strongly depends on the quantity of deposited  $\text{As}_2\text{S}_3$ . The greater film thickness, the larger the mean grain size. Most likely the coalescence is taking place during the film growth. It seems that the thickness driven evolution of a-  $\text{As}_2\text{S}_3$  films obeys the rule similar to that known as Oswald ripening [6, 7]. For our films we don't observe the increase of main period of surface quasigratings with the increase of films' thickness. Quite the reverse is taking place - some decrease of the main period with the increase of films' thickness has been observed. Besides, for our films the surface granularity has manifested itself stronger in thinner films as the background over which the ordered structure is formed. So, our regularities don't coincidence with such scenario.

Another possible cause of self-ordered surface relief may be the surface instability of stressed solid. Many of the thin films have large residual stresses due to their growth processes or lattice mismatch. The internal stress in amorphous film may be due to several processes: incorporation of atoms (e.g. residual gas), chemical reactions such as oxidation, microscopic voids, etc. [15-17]. It is the known fact that the thermally deposited at normal vapor incidence angle  $\text{As}_2\text{S}_3$  films are compressively stressed [18]. The initial stress is evenly distributed across the film depth, and its value is  $\sim 10$  Mpa [19].

Stress can greatly affect surface evolution. It is well known that elastic relaxation drives morphological instability of film surface and results in non-planar film. The instability can manifest itself in the formation of

the wavy shape on the surface, surface ripples, cusps, and island-like mounds (quantum dots and quantum wires). This stress-driven morphological instability has been studied extensively. In this case, the basic mechanism of the pattern formation is related to the Asaro–Tiller–Grinfeld (ATG) instability [20–22], which predicts the morphological instability of the uniaxially stressed solid interface due to surface diffusion or melting and recrystallization.

Relatively long-wave perturbations of the interface lead to the reduction of the system's elastic energy, whereas shortwave corrugations are hampered by surface energy. Competition between surface energy and strain energy leads to the critical wavelength of surface roughening. From the linear stability analysis of the sinusoidal perturbation, the critical wavelength is [22, 23]

$$d_c = \pi \gamma_s E / \{(1-\nu^2) \sigma_0^2\} \quad (1)$$

where  $\gamma_s$ ,  $E$  and  $\nu$  are material constants, representing surface energy, Young's modulus and Poisson ratio of the thin film, respectively. The  $\sigma_0$  is the residual stress when the film is perfectly flat.

Let us estimate the critical wavelength of surface roughening for normally deposited  $\text{As}_2\text{S}_3$  films, using the  $\sigma_0$ ,  $E$ ,  $\nu$  data from [18, 19, 24]:  $\sigma_0 = 10 \text{ Mpa}$ ,  $E = 1 \cdot 10^{10} \text{ Pa}$ ,  $\nu = 0.3$ . The surface energy estimate is  $\gamma_s \sim 1 \text{ N/m}$  [25]. For the above values of the parameters the estimate for  $d_c$  is  $\sim 1 \text{ mm}$ . Thus, for normally deposited  $\text{As}_2\text{S}_3$  films the very smooth and stretched long wavelength surface modulation is expected. This kind of modulation is very difficult to observe due to its wavelength exceeding the relief height by several orders of magnitude. It is not surprising that we did not succeed in detecting such modulation in the normally deposited  $\text{As}_2\text{S}_3$  films.

The paper [7] provides the only available data on the mechanical properties of  $\text{As}_2\text{S}_3$  ODF. The microhardness of such films is several times lower as compared to  $\text{As}_2\text{S}_3$  NDF. The same is true for the Young's modulus of  $\text{As}_2\text{S}_3$  ODF. The increase in compliance (decrease in stiffness) of  $\text{As}_2\text{S}_3$  ODF can be attributed to greater porosity. Another possible cause may be the phase separation similar to  $\text{GeSe}_2$  films deposited at high obliqueness angles ( $\beta \sim 60^\circ - 80^\circ$ ) [26]. The latter films consist of the Ge-rich columns phase and the intercolumnar Se-rich phase. Due to this decrease of Young's modulus the difference between measured ( $\sim 0.2 \mu\text{m}$ ) quasigrating period values and those computed using formula (1) ( $\sim 200 \mu\text{m}$ ) drops  $\sim 1000$  times.

Assuming that the observed quasigrating surface relief of  $\text{As}_2\text{S}_3$  ODF is due to the ATG instability, then the decrease of the surface modulation wavelength in  $\text{As}_2\text{S}_3$  ODF as compared to normally deposited  $\text{As}_2\text{S}_3$  films by 1000 times should be explained by a much bigger stress in them.

It is known that ambient atmosphere influences on the proceeding of physico-chemical processes in chalcogenide films [see, for example, [27, 28]. This influence is first of all connected with oxygen, the most common and active element of environment. In chalcogenide ODF this influence is stronger due to the lower density of these films [5]. The processes should run with greater intensity in the near-surface part of the films. Authors [19] found that for normally deposited  $\text{As}_2\text{S}_3$  film the aging under ambient conditions results in the change of stress distribution across film thickness. It significantly increases on the outer surface and decreases inside the film. Such stress redistribution across film thickness indicates the different way the relaxation processes run in the near-surface and deeper inside the film.

Thus, upper near-surface area of obliquely deposited  $\text{As}_2\text{S}_3$  film should be stiffer and more stressed. At the same time, the pronounced columnar structure of the main part of these films provides a lot of free space where the bond breaking and atomic movements are facilitated. This part of the films may be rather plastic. So, one can expect that from the mechanical point of view the obliquely deposited  $\text{As}_2\text{S}_3$  films are similar to human skin, which consists of the relatively stiff epidermis attached to the soft dermis that is ten times as thick. That is why the action of stresses may result in wrinkling of the film, similar to wrinkling of human skin [29, 30].

Indeed, thin films bonded to compliant substrates often develop wrinkles when subjected to an applied or inherent compressive stress [31, 32]. Stiff skin forms on surface areas of a flat polydimethylsiloxane (PDMS) upon exposure to focused ion beam or UV/ozone treatment leading to ordered surface wrinkles [31–34]. Similar wrinkling pattern has also been observed in other systems, such as thermally grown oxides on metals [35–37] and thin metal films on polymers [31, 38]. Therefore, the considerations developed for human skin may be applicable to thin films.

We estimated the relations between mechanical properties of upper stiffened and lower compliant parts of  $\text{As}_2\text{S}_3$  ODF with the help of the theory describing the behavior of stressed stiff elastic layer on compliant elastic substrate [29-33]. The estimated values are:

Thickness of the upper modified part of the films is 15-20 nm. Its elastic modulus value exceeds the one for the lower non-modified (main) part of the films by more than one order of magnitude.

In conclusion, let us consider the possible practical aspects of this study. Modern technology has developed a broad range of applications with integrated hard and soft materials at micron to nanometer scales. The technology usually requires the films to be flat with no wrinkles. Typically, wrinkling of thin films has been treated as a nuisance to be avoided [39, 40] rather than an exquisite pattern to be exploited. However, once understood, it is possible to control and even use wrinkling, for example, to develop stretchable interconnects for flexible electronics [41], [42], tunable diffraction gratings [43], force spectroscopy in cells [44], biocompatible cell and particle alignment [45], and advanced metrology methods [46]. The formation and control of the ordered pattern may find uses in optical devices as diffraction gratings and microfluidic devices in making channels with microstructured walls. The films with regular and well oriented wrinkles can be used as cladding layer for flat waveguides with grating input-output couplers of light beams.

## 5. Conclusions

Surface morphology and optical characteristics of the oblique deposited  $\text{As}_2\text{S}_3$  films was analyzed using the data on AFM and multi-angle ellipsometric investigation.

The AFM has revealed the details of the surface relief of obliquely deposited films showing quasi-regular grating-like structure, with the spatial frequency of quasi-gratings being in the  $500\text{-}6000\text{ mm}^{-1}$  range, and relief depth in the 1-60 nm range. It was found that the wrinkling (rippling) phenomenon in obliquely deposited  $\text{As}_2\text{S}_3$  films is dependent first of all on the thickness of the films. Ordering degree also depends on the substrate. The preliminary deposition of thin Cr film on the glass substrate results in more pronounced surface self-ordering of obliquely deposited  $\text{As}_2\text{S}_3$  films.

Average refractive indexes values of oblique deposited  $\text{As}_2\text{S}_3$  films calculated from multiangle ellipsometric measurements within the framework of "isotropic uniform layer model" are  $\sim 2\%$  lower compared to the values of refractive indexes of  $\text{As}_2\text{S}_3$  films obtained using the normal (perpendicular) deposition. With the increase of the film thickness the refractive index of the obliquely deposited  $\text{As}_2\text{S}_3$  film decreases.

Most probable explanation for the observed effect is the near-surface stress that plays significant role in the self-organized ordering of nanostructures at the mesoscopic length scales (several nm – hundreds of nm). Due to the structural anisotropy of the obliquely deposited  $\text{As}_2\text{S}_3$  films, the stress forces are also anisotropic. As a result, a set of wrinkles perpendicular to the direction of compressive field is formed.

The effect is the cheap and easy way to create quasi-gratings on the surface of amorphous chalcogenide films, and could be used for fabrication of nano- and micro-devices.

## References

- [1] B. Singh, S. Rajgopalan, P.K. Bhat, D.K. Pandya, K.L. Chopra, *Solid State Commun.* **29**, 167 (1979).
- [2] S. Rajgopalan, K.S. Harshvardhan, L.K. Malhotra, K.L. Chopra, *J. Non-Cryst. Solids* **50**, 29 (1982).
- [3] P. K. Gupta, K. L. Chopra. *Appl. Phys. A: Mater.s Sci. Proc.* **46**, 103 (1988).
- [4] F. Jensen. *Thin Solid Films* **78**, 15 (1981).
- [5] C. A. Spence, S. R. Elliot. *Phys. Rev.* **B 39**, 5452 (1989).
- [6] N. Starbov, K. Starbova, J. Dikova. *J. Non-Cryst. Solids* **139**, 222 (1992).
- [7] K. Starbova, J. Dikova., N. Starbov. *J. Non-Cryst. Solids* **210**, 261 (1997).
- [8] J. Dikova, P. Sharlandjiev, P. Gushterova, Tz. Babeva. *Vacuum* **69**, 395 (2003).
- [9] J. Dikova, Tz. Babeva, P. Sharlandjiev. *J. Optoelectr. Adv. Mater.* **7**, 361 (2005).
- [10] Y. Kuzukawa, A. Ganjoo, K. Shimakawa. *J. Non-Crystall. Solids* **227–230**, 715 (1998).
- [11] P. Bhardwaj, P. K. Shishodia, R. M. Mehra. *J. Optoelectr. Adv. Mater.* **3**, 319 (2001).
- [12] P. Bhardwaj, P. K. Shishodia, R. M. Mehra. *J. Mater. Sci.* **42**, 1196 (2007).
- [13] I. Z. Indutnyy, I. Yu. Maidanchuk, V. I. Min'ko, P. E. Shepeliavyi, V. A. Dan'ko.

- J. Optoelectr. Adv. Mater. **7**, 1231 (2005).
- [14] H. J. Leamy, A. G. Dirks. J. Appl. Phys. **49**, 3430 (1978).
- [15] W. Backel. J. Vac. Soc. Techn. **6**, 606 (1969).
- [16] E. A. Hill and G. R. Hoffman. Br. J. Appl. Phys. **18**, 13 (1967).
- [17] L. Eckertova, in Physics of Thin Solid Films (Plenum-Press, 1986) pp 202-210.
- [18] M. L. Trunov, Yu.B. Gvardionov. Sov J Izmeritel'naya Technika **N10**, 22 (1989). (In Russian); M. L. Trunov, A. G. Anchugin, N. D. Savchenko. J. Sci. Appl. Photogr. Cinematogr. **5**, 384 (1991) (in Russian).
- [19] N.D. Savchenko, T.N. Shchurova, N.Yu. Baran, A.A. Spesivkykh. Vacuum **80**, 128 (2005).
- [20] R.J. Asaro, W.A. Tiller. Metall. Trans. **3**, 1789 (1972).
- [21] M.A. Grinfel'd, Sov. Phys. Dokl. **31**, 831 (1986).
- [22] D.J. Srolovitz. Acta Metall. **37**, 621(1989); W.H. Yang, D.J. Srolovitz, Phys. Rev. Lett. **71** 1593 (1993).
- [23] Z. Liu, H.-H. Yu. Thin Solid Films **513**, 391 (2006).
- [24] T. N. Shchurova, N. D. Savchenko. J. Optoelectr. Adv. Mater. **3**, 491 (2001).
- [25] D. Sander. Current Opinions Solid State Mater. Sci. **7**, 51 (2003).
- [26] P. Boolchand, Mingji Jin, D. I. Novita, S. Chakravart. J. Raman Spectrosc. **38**, 660 (2007).
- [27] M. V. Sopinsky, M. T. Kostyshin. J. Optoelectr. Adv. Mater. **3**, 411 (2001).
- [28] M. V. Sopinsky, P. E. Shepeliavi, A. V. Stronski, E. F. Venger, J. Optoelectr. Adv. Mater. **7**, 2255 (2005).
- [29] E. Cedra, L. Mahadevan. Phys. Rev. Lett. **90**, 074302-1 (2003).
- [30] F. Brochard-Wyart, P.G. de Gennes. Science **300**, 441 (2003).
- [31] N. Bowden, S. Brittain, A. G. Evans, J. W. Hutchinson, G. M. Whitesides. Nature (London) **393**, 146 (1998).
- [32] R. Huang, S.H. Im. Phys. Rev. **E 74**, 026214 (2006).
- [33] M.-W. Moon, S. H. Lee, J.-Y. Sun, K. H. Oh, A. Vaziri, J. W. Hutchinson. doi:10.1073/pnas.0610654104. PNAS published online Jan 16, 2007.
- [34] K. Efimenko, W.E. Wallace, J. Genzer. J. Colloid. Interf. Sci. **254**: 306 (2002).
- [35] Z. Suo. J. Mech. Phys. Solids **43**, 829 (1995);
- [36] V. K. Tolpygo, D. R. Clarke. Acta Mater. **46**, 5153 (1998).
- [37] V. K. Tolpygo, D. R. Clarke. Acta Mater. **46**, 5167 (1998).
- [38] W. T. S. Huck, N. Bowden, P. Onck, T. Pardo, J. W. Hutchinson, G. M. Whitesides, Langmuir **16**, 3497 (2000).]
- [39] F. Iacopi, S.H. Brongersma, K. Maex. Appl. Phys. Lett. **82**, 1380 (2003).
- [40] H Yin, R. Huang, K.D. Hobart, J. Liang, Z. Suo, S. R. Shieh, T.S Duffy, F.J Kub, J.C. Sturm. J. Appl. Phys. **94**, 6875 (2003).
- [41] M. Watanabe, H. Shirai, T. Hirai. J. Appl. Phys. **92**, 4631. (2002).
- [42] S.P Lacour, S. Wagner, Z.Y. Huang, Z. Suo. Appl. Phys. Lett. **82**, 2404 (2003).
- [43] C. Harrison, C. M. Stafford, W.H. Zhang, A. Karim. Appl. Phys. Lett., **85**, 4016 (2004).
- [44] A.K. Harris, P. Wild, D. Stopak. Science **208**, 177 (1980).
- [45] K. Efimenko, M. Rackaitis, E. Manias, A. Vaziri, L. Mahadevan, J. Genzer. Nature Mater. **4**, 293 (2005).
- [46] C. M. Stafford, B. D. Vogt, C. Harrison, D. Julthongpiput, R. Huang. Macromolec. **39**, 5095 (2006).